Characterization of Human Metal Model ESD Based on Radiated Susceptibility

Hamed Kajbaf[1], Jin Min[2]
Amber Precision Instruments (API)
[1]hamed, [2]jinmin@amberpi.com

***Abstract*–The radiated susceptibility of electronic boards to human metal (HMM) model electrostatic discharge (ESD) is studied. A circuit and a full-wave simulation model of the HMM ESD generator is developed and verified by measured data to investigate the coupling mechanism between the generator and a microstrip line. The coupling mechanism is compared with that of a near-field probe excited by a transmission line pulser (TLP). The coupled waveform shows to have a good agreement. A scalable empirical formula is derived to correlate the voltage setting of HMM ESD generator and TLP for equivalent coupled waveform.**

Keywords – ESD, HBM, HMM, radiated emissions, radiated susceptibility, near-field, TLP.

1. INTRODUCTION

It has been well known that an electrostatic discharge (ESD) initiated by assembling personnel, charged components, charged tools, and end users may cause failure by overstressing electronic components [1]. Depending on the electrical properties and geometry of the surrounding materials, as well as the properties of the medium between the materials (usually air), an electric arc might occur at a distance that satisfies the Paschen's law (under a homogeneous electric field condition) [2]. The electric arc creates a plasma channel between the two materials by ionizing the medium which facilitates the transfer of electrons and consequently creates a current flow. Even though the discharge is initiated from an electrostatic source, the current flow is an electrodynamic phenomena with a waveform depending on the surrounding materials and the conditions of the medium.

Various standardized tests has been developed by the ESD community to help the designers with evaluating the electronic components, printed circuit board (PCB) assemblies, and electronic devices. Even though ESD tests are usually categorized as conducted susceptibility tests (such as MIL-STD-461G CS118), they inherently have radiated susceptibility (RS) nature as well, caused by the electrodynamics of the discharge. ANSI/ESD SP14.5-2015 is developed by ESD Association (ESDA) as the standard practice to help the designers with testing components as well as devices for immunity to near-field coupling or radiated emissions (RE) from an ESD event using near-field probes [3]. This test may be used for component-level evaluation for hard failure or system-level evaluation for hard or soft failure.

Component-level ESD standards such as human body model (HBM) defined in ANSI/ESDA/JEDEC JS-001-2010 or MIL-STD-883J Method 3015.9 evaluate the susceptibility level of the components on an isolated test board [4]. On the other hand, device or system-level standards such IEC 61000-4-2 or ANSI/ESD SP5.6-2009 evaluate the susceptibility of the system for hard or soft failure in a PCB assembly [5]. These tests are usually referred to as human metal model (HMM) with some variations in different standards [6]. Under many design conditions, component-level robustness to ESD test does not necessarily guarantee a successful system-level test. The HMM ESD standard per ANSI/ESD SP5.6-2009 is specifically developed for testing electronic components in an attempt to increase system-level success rate once the components are used in an assembled board. However, due to the complexity of system-level failure mechanisms, the inherent RS characteristics of the system-level standards are not well explored and are not fully compared with near-field characteristics of standards such as ANSI/ESD SP14.5-2015.

In this paper, the coupling mechanism between an ESD generator used for IEC 61000-4-2 test and a matched microstrip line is studied. The victim components in this simplified system-level test scenario are resistive terminations of the microstrip line. On the other hand, the coupling mechanism between near-field injection probe used for ANSI/ESD SP14.5-2015 and the microstrip line is investigated. A set of simulations and measurements are performed to quantify these coupling mechanisms based on the voltage developed across the terminations.

The full-wave simulation of ESD generator is prepared and evaluated based on discharge current under standard load condition per IEC 61000-4-2. The simulation is then used to study the near-field attenuation of the field caused by electrodynamics of the ESD generator. The coupled waveform to the microstrip is compared with that of near-field magnetic probe excited by a transmission line pulser (TLP) on the same structure. An empirical equation is

then derived for a microstrip line structure to correlate the equivalent voltage setting of the TLP and the ESD generator.

2. ESD WAVEFORM

The waveform of ESD generator is usually characterized by the current or voltage waveform on a standardized load. If the standard load is replaced by a component or device under test (DUT), the waveform will change based on the input impedance of the DUT and output impedance of the generator. To compare the waveform of various standards, the circuit models of ESD generators are developed in SPICE for HBM, HMM, and TLP models. Additionally, the full-wave model of HMM ESD generator is developed in CST Studio Suites for studying the radiated emissions.

2.1 HBM

As a reference for comparison with component-level tests, a SPICE model is developed which takes into account the main RC network and the parasitic components to achieve the standard current waveform specified in ANSI/ESDA/JEDEC JS-001-2010. The human body is modeled as a 100 pF capacitor charged to the intended voltage level and then discharged to the DUT through a 1500 Ω resistor. This RC network is representative of a person touching electronic component with bare hand. There are other parasitic components involved in the instrumentation of the ESD generator [1,3]. The model is then verified under two standard load condition at 2 kV; a short and a 500 Ω resistor.

2.2 HMM

The HMM is modeled as a 150 pF capacitor charged to the intended voltage level and then discharged to the DUT through a 330 Ω resistor. The RC network is representative of a person touching a device with a handheld metal part. A SPICE model for the ESD generator is developed and tested under 2 Ω resistor. The first ~6 ns of the current is mainly created by parasitic components of the ESD generator tip and the next tens of nanoseconds are dominantly formed by the main RC network [4]. Additionally, the ESD generator is modeled in 3D full-wave details to analyze the RE. Figure 1 compares the simulated and measured current waveform of a 2 kV pulse through 2 Ω resistor with ideal waveform per IEC 61000-4-2.

2.3 TLP

TLP is conventionally used to characterize the I-V curve of electronic components under ESD conditions. A transmission line, with the length proportional to pulse width, is charged to the intended voltage and then discharged to the DUT. In this study, the TLP is used to inject pulse into a near-field probe as in ANSI/ESD SP14.5-2015 standard practice. The circuit model of the TLP is developed in SPICE and the voltage waveform of 2 kV pulse across a 50 Ω resistor is compared with measured data as shown in Fig. 2.

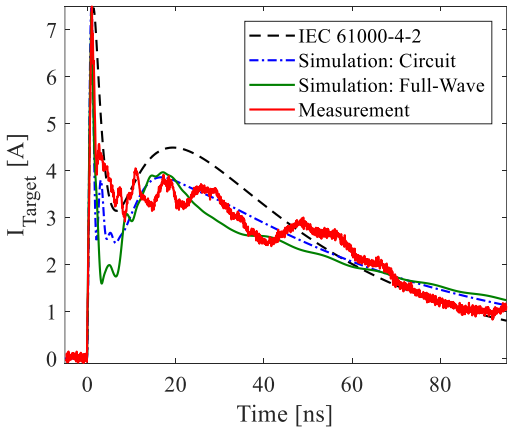

Fig. 1 Simulation and measurement of ESD generator current waveform.

The TLP used for this study is API AT-8000DA which has ~500 ns rise time (10%-90%). This TLP is designed to work with near-field probes and therefore has higher rise time compared to IEC 61000-4-2 waveform. Two probe are used for this study which are magnetic field probes with 2 mm by 2 mm (Hx2) and 5 mm by 5 mm (Hx5) square shape loop dimension. The probe induces current on the DUT and the induced current on DUT is proportional to derivative of the injected waveform. The TLP is designed to have a slow fall time to avoid double pulse per injection through the near-field probe [7,8].

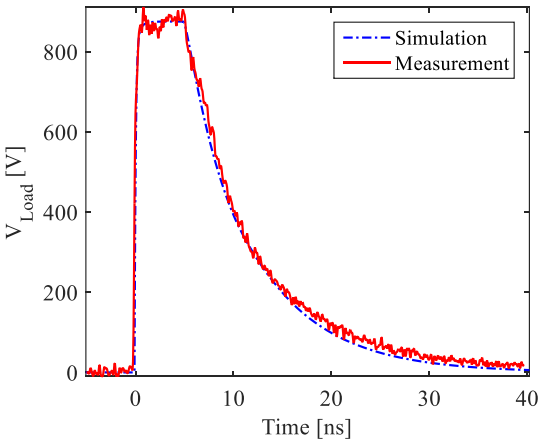

Fig. 2 Simulation and measurement of TLP voltage waveform.

Since the waveforms of HBM, HMM, and TLP generators are designed for different applications and characterized differently, they are not typically compared to each other directly. However, to have a better understanding of relative magnitude of injected pulses, the current passing through a 2 Ω resistor is simulated using the SPICE model of these generators

as shown in Fig. 3. The difference between the peak magnitudes of the current waveforms is mainly due to the series resistance in the generators' discharge path and the parasitic components of the generator.

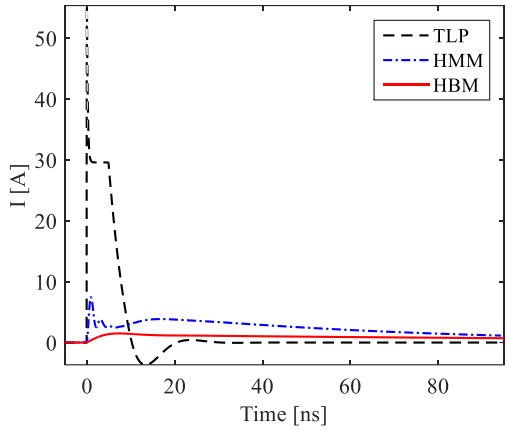

Fig. 3 Comparison between simulation of TLP, HMM, and HBM current waveform passing through 2 Ω load at 2 kV setting.

3. ESD: RADIATED SUSCEPTIBILITY

To study the RE from the HMM ESD generator, the full-wave simulation is created based on the model presented in [9,10] and is then modified to fit Noiseken or EMTest ESD generators. The contact discharge tip of the modeled ESD generator is placed at 10 mm away from a 50 Ω microstrip line. The microstrip board dimensions are 100 mm by 100 mm. The ESD generator is injecting into a conductive sheet which is representing the horizontal coupling plane (HCP). The microstrip is elevated from the HCP with no conductive path between the two. The signal line of the microstrip is aligned with the ESD generator tip, as shown in Figure 4, and is terminated to microstrip ground layer using 50 Ω resistors at both ends. The simulated ESD generator is excited by 2 kV step pulse (representing relay action in physical ESD generator). The IEC 61000-4-2 waveform is simulated by 3D geometrical and lumped element components in the full-wave model. The magnetic and electric field is monitored on top of the microstrip at 1 mm away from the top layer. Additionally, the voltage and current of the 50 Ω terminations are monitored which are representing victim electronic components on a PCB.

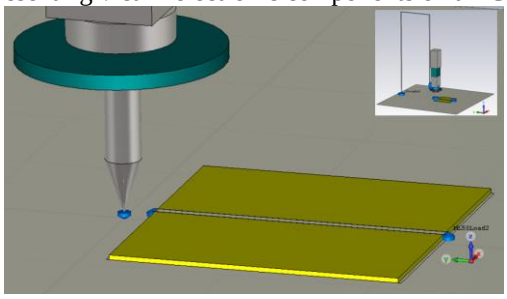

Fig. 4 Full-wave simulation model of HMM ESD generator and a 50 Ω microstrip line. ESD injection is on HCP.

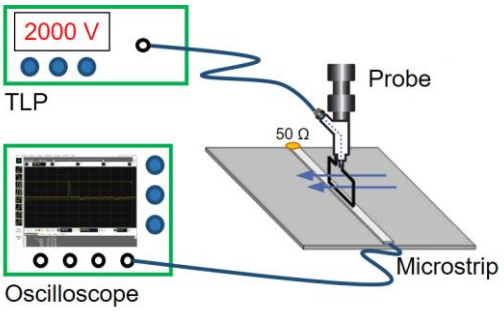

Fig. 5 Measurement setup for near-field injection using TLP.

A measurement setup is prepared to study the near-field coupling to microstrip per ANSI/ESD SP14.5-2015 standard practice. The magnetic field probes are individually placed on top of the 50 Ω microstrip with the field lines normal to the signal line for maximum coupling as shown in Fig. 5. The probes are then excited with TLP at 2 kV setting. The microstrip is terminated on one end using 50 Ω and is connected to an oscilloscope on the other end to monitor the coupled voltage. The distance between the probe tip and signal line is 1.4 mm.

The magnitude of the induced current from ESD generator on the matched microstrip used in this study is a function of multiple factors: ESD generator voltage setting, horizontal distance between the microstrip and contact discharge tip, the elevation of microstrip above HCP, and the orientation of the microstrip. On the other hand, the induced current on the matched microstrip from the near-field probe excited with TLP is a function of the following factors: the TLP voltage setting and waveform, the probe distance to the microstrip signal line, probe type (magnetic or electric), and probe factor.

The relationship between the applied voltage to the near-field probe and the field developed at the tip of the probe is defined as the probe factor. The probe factor of an ideal loop probe can be calculated from

$$PF = \frac{1}{2\pi\mu_0 f A_{ef}} \tag{1}$$

where, f is frequency and A_{ef} is the effective area of the probe [11]. To make the coupled waveform to microstrip comparable between probes with different sizes, one needs to take into account the probe factor as well as the electrical height of the probe above the signal line. Since the microstrip is in the near-field of the probe, the relationship between the electrical height and free-space attenuation is nontrivial. Based on empirical data, the free-space near-field attenuation for the probes used for this study are proportional to $\sim 1/r^{1.66}$, where r is distance from the electrical center of the probe to the signal line.

For a spark-less discharge using contact discharge method, the dominant nonlinearity for predicting the RE from HMM ESD generator and correlating it with near-field probe injections are the near-field effects of the ESD generator. Therefore, the magnetic field normal to microstrip line (H_x) are monitored in the simulation and are shown in Fig. 6. The free-space near-field attenuation of the HMM ESD generator close to the microstrip line is then calculated to be proportional to ~$1/R^{1.25}$, where R is the distance from ESD generator tip to an observation point on top of the microstrip.

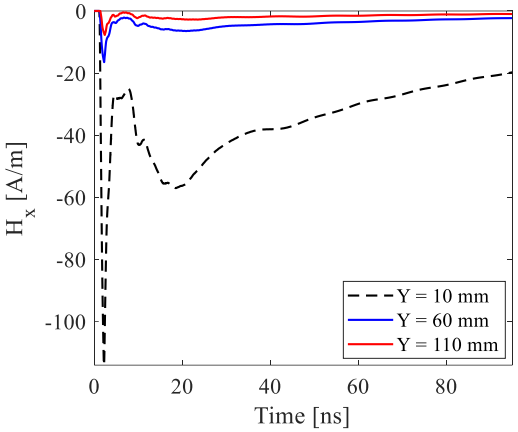

Fig. 6 Simulated magnetic field normal to microstrip line (H_x) at different distances from ESD generator tip.

The near-field attenuation factors derived in this study are considered to be estimates and some simplification are included in the derived numbers. However, they can be practically used for deriving an engineering correlation between field induced by HMM ESD generator and TLP injection using near-field probe. The following formula is then derived based on simulated and measured data on a matched microstrip line

$$V_{eq} = \frac{1.98 \times V_{ESD}}{A_{ef}} \left(\frac{r}{2.4} \right)^{\alpha} \cdot \left(\frac{60}{R} \right)^{\beta} \qquad (2)$$

where, V_{eq} is the equivalent voltage setting on TLP, V_{ESD} is the HMM ESD generator voltage setting, r is the distance from the electrical center of the probe to the signal line, R is the distance from the center of microstrip to tip of HMM ESD generator in mm, α is 1.66, and β is 1.25. The values of α and β are from the near-field analysis of the ESD generator and near-field probes.

Figure 7-a compares the simulated voltage waveform across 50 Ω termination on the far-end of the microstrip line (black curve) and the measured voltage on the microstrip line injected with Hx2 probe (blue curve) and Hx5 probe (red curve). It can be seen from this figure that the waveforms have similar pattern with different magnitudes.

To check the validity of the derived formula for different near-field probes, the correction factor for the equivalent TLP voltage is applied to waveforms of Fig. 7-a and are compared to HMM simulations in Fig. 7-b. It can be seen that a good correlation is observed between the waveforms after applying the correction factor.

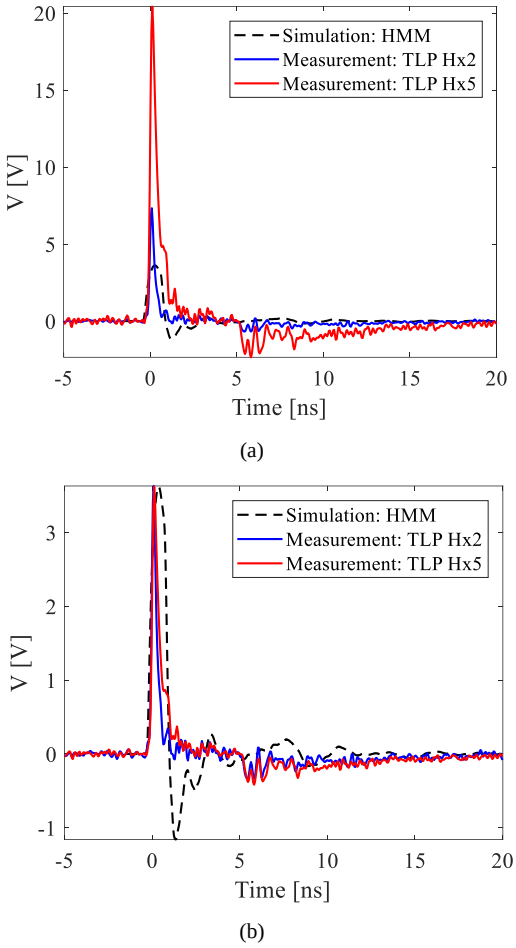

Fig. 7 Comparison between simulation of HMM and measurement of TLP waveform coupled to microstrip line (a) with no correction factor and (b) with correction factor.

4. CONCLUSION

In this paper, HMM ESD generator based on IEC 61000-4-2 are successfully simulated using circuit and full-wave models. The radiated susceptibility of a microstrip board to the emissions from ESD generator is then studied using the full-wave simulation model. The coupling mechanism between ESD generator and the microstrip is then compared with that of a measurement setup per ANSI/ESD SP14.5-2015. The coupled waveforms to microstrip line resulted from the two methods show to have a good agreement. An empirical conversion formula is derived which correlates the voltage setting on an HMM ESD generator and the voltage setting of a TLP for a microstrip line. Additionally, the current waveform of the HBM, HMM, and TLP are simulated and verified

by measurement for better comparison.

The main focus of this study is the coupling mechanism of ESD to microstrip line. More complex electronic boards with nonlinear components and protection circuits would require more thorough investigation of the coupling mechanism and/or a statistical analysis [12]. In case of an arc discharge, the nonlinear and time varying physics of the plasma channel need to be included in the simulation models [13].

5. ACKNOWLEDGMENT

The authors would like to thank Dr. David Pommerenke and Kimpsion Corporation for providing valuable feedback for this paper.

REFERENCES

[1] S. Frei, D. Pommerenke, and B. Arndt, “High-voltage coupling in electronic devices and control units,” *FAT 249*, Feb. 2013.

[2] S. Bönisch *et al.*, “Modeling of short-gap ESD under consideration of different discharge mechanisms,” *IEEE Trans. Plasma Science*, vol. 31, no. 4, pp. 736-744, Aug. 2003.

[3] *Standard Practice for Electrostatic Discharge Sensitivity Testing – Near Field Immunity Scanning - Component/Module/PCB Level*, ANSI/ESD SP14.5-2015.

[4] *Human Body Model (HBM) - Component Level*, ANSI/ESDA/JEDEC JS-001-2010.

[5] *Testing and Measurement Techniques – Electrostatic Discharge Immunity Test*, IEC 61000-4-2, 2008.

[6] J. Baran and J. Sroka, “Human-metal electrostatic discharge in IEC, ANSI and MIL standards,” *Interference Technology*, Sep. 2011.

[7] D. Pommerenke *et al.*, “Application and limits of IC and PCB scanning methods for immunity analysis,” in *Proc. 18th Int. Zurich Symposium on EMC*, Munich, 2007, pp. 83-86.

[8] G. Muchaidze *et al.*, “Susceptibility scanning as a failure analysis tool for system-level electrostatic discharge (ESD) problems,” *IEEE Trans. Electromagn. Compat.*, vol. 50, no. 2, pp. 268-276, May 2008.

[9] S. Caniggia and F. Maradei, “Circuital and numerical modeling of electrostatic discharge generators,” *40th IAS Annual Meeting, Conference Record of the 2005 Industry Applications Conference*, 2005, pp. 1119-1123.

[10] J. Xiao *et al.*, “Model of secondary ESD for a portable product,” *IEEE Trans. Electromagn. Compat.*, vol. 54, no. 3, pp. 546-555, June 2012.

[11] C.F.M. Carobbi and L.M. Millanta, “Analysis of the common-mode rejection in the measurement and generation of magnetic fields using loop probes,” *IEEE Trans. Instrum. and Meas.*, vol. 53, no. 2, pp. 514-523, April 2004.

[12] J. Xiao *et al.*, “Local probe injection compared to direct ESD injection,” *EMC Compo*, France, Nov. 2009.

[13] D. Liu, “Full wave simulation of an electrostatic discharge generator discharging in air discharge mode into a product and quantify channel performance utilizing novel time domain convolution method,” M.S. thesis, Dept. Elect. Comp. Eng., Missouri Univ. Science and Technology, Rolla, MO, 2010.